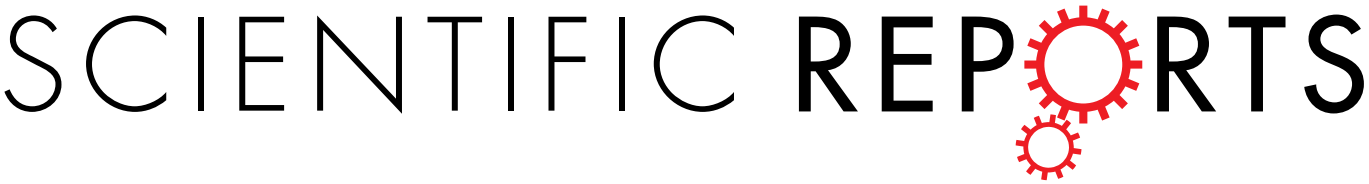

OPEN

Broadband suppression of backscattering at optical frequencies using low permittivity dielectric spheres

Received: 19 July 2017
Accepted: 20 October 2017
Published online: 07 November 2017

M. Ismail Abdelrahman[1,2], C. Rockstuhl[1,3] & I. Fernandez-Corbaton[3]

The exact suppression of backscattering from rotationally symmetric objects requires dual symmetric materials where $\varepsilon_r = \mu_r$. This prevents their design at many frequency bands, including the optical one, because magnetic materials are not available. Electromagnetically small non-magnetic spheres of large permittivity offer an alternative. They can be tailored to exhibit balanced electric and magnetic dipole polarizabilities $a_1 = b_1$, which result in approximate zero backscattering. In this case, the effect is inherently narrowband. Here, we put forward a different alternative that allows broadband functionality: Wavelength-sized spheres made from low permittivity materials. The effect occurs in a parameter regime where approximate duality is met for all multipolar order $a_n \approx b_n$, in a weakly wavelength dependence fashion. In addition, and despite of the low permittivity, the overall scattering response of these spheres is still significant. Scattering patterns are shown to be highly directive across an octave spanning band. The effect is analytically and numerically shown using the Mie coefficients.

The scattering of light upon interacting with matter is a central problem in electromagnetism which is relevant in many branches of physics such as nuclear physics, astrophysics, and spectroscopy. The theory of plane wave scattering from spheres was developed more than a century ago by Gustave Mie[1]. Due to the intricate nature of the multiple phenomena taking place in this interaction process, the exploration of different regimes continues to disclose surprising new effects that have a profound impact on a wide range of applications[2–5]. A referential example is the desire to suppress the backscattering from spheres that could find use, e.g. in light management structures used in photovoltaic devices[6–8] and laser tractor beams (negative optical force)[9]. In 1983 Kerker *et al.*[10] showed that it is possible to achieve zero backscattering (ZBS) in a direction opposite to the illumination using spheres made from a dual material[11], i.e. a material with identical electric permittivity and magnetic permeability $\varepsilon_r = \mu_r$. Electromagnetic duality implies the equal complex amplitude excitation of electric and magnetic multipolar moments inside the sphere. Their scattered fields interfere destructively in the backward direction. The condition of spherical symmetry can be relaxed to cylindrical symmetry[12] and even to discrete rotational symmetries[13]. However, no natural material with magnetic properties exists at optical frequencies. In other words, all materials exhibit a permeability of $\mu_r = 1$. Thus, Kerker's method can not be applied at optical frequencies. While metamaterials might be an avenue to solve this problem, there has been no report of a dual metamaterial so far. Moreover, the absorption inherent to the resonant inclusions needed to achieve an effective permeability larger than one would likely spoil the entire effect.

Nevertheless, it has been shown, both experimentally[14] and theoretically[15,16], that it is possible to excite a notable magnetic dipole moment at optical frequencies in nanospheres made from a high permittivity dielectric material where intrinsic losses can be negligible. When the radius and permittivity of small spheres are carefully selected, it is possible to achieve duality in the dipolar approximation[17], albeit for a very narrow spectral region. This leads to the possibility of approaching ZBS in experiments, as shown in ref.[18] in the GHz band, and ref.[19] in the optical band. Dielectric spheres of moderate permittivity can also exhibit forward scattering at their scattering peak in the visible region[20]. Zero backscattering has also been experimentally approached in the optical band

[1]Institute of Theoretical Solid State Physics, Karlsruhe Institute of Technology, Karlsruhe, Germany. [2]Aix Marseille Univ, CNRS, Centrale Marseille, Institut Fresnel, Marseille, France. [3]Institute of Nanotechnology, Karlsruhe Institute of Technology, Karlsruhe, Germany. Correspondence and requests for materials should be addressed to M.I.A. (email: m.abdelrahman@fresnel.fr)

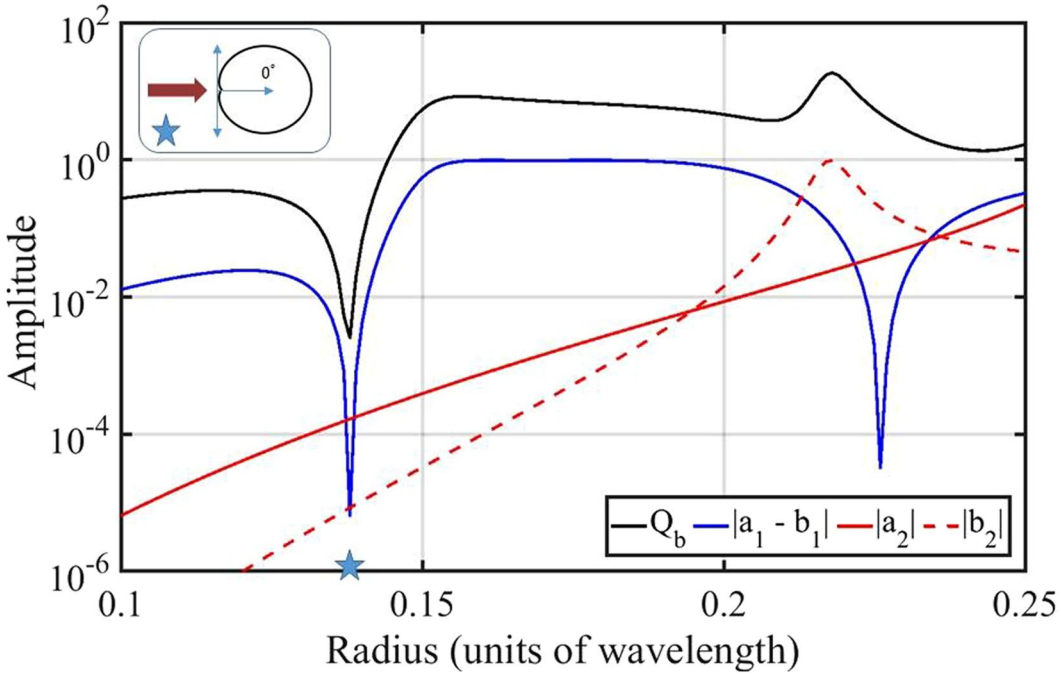

Figure 1. Backscattering efficiency Q_b of a nonmagnetic sphere with permittivity $\varepsilon_r = 10$ as a function of radius in units of wavelength λ_0. At $r = 0.138\,\lambda_0$, the electric and magnetic dipoles are balanced ($a_1 = b_1$), and the scattering pattern resembles a Huygens source, as shown in the top-left corner. The figure shows another point where $a_1 = b_1$ at $r = 0.226\,\lambda_0$, however, this larger sphere exhibits considerable backscattering due to the notable excitation of high order multipoles.

using electromagnetically small cylindrical objects[21]. Arrays of silicon disks have been used to design near-unity transmission Huygens's surfaces under normal illumination in an extended spectral region[22,23]. As the size of the objects grows, higher order multipoles become significant and, while they can be used for ZBS interference in some cases[24,25], they are a source of duality breaking and ZBS degradation in homogeneous spheres. This is illustrated in Fig. 1. Consequently, achieving a broadband ZBS from spheres at optical frequencies remains elusive.

The basic problem can be formulated quite simply: Can we design a broadband strongly scattering object with a heavily reduced backscattering? In this article, we show that the answer is positive for electromagnetically large dielectric spheres made from low permittivity materials that, if carefully designed, exhibit both ZBS and strong interaction in an extended spectral domain. Low permittivity materials are being widely used in various applications[26]. We explain the underlying physics by analytical means and corroborate our findings with calculations based on Mie coefficients, assuming a plane wave illumination. To quantify the relevant features and to analytically motivate the chosen path, we consider the backscattering efficiency Q_b as a parameter to judge the backscattering characteristics of spheres of arbitrary sizes. The backscattering efficiency is a unitless quanitity that is directly related to the fraction of energy scattered in the backward direction ($\theta = 180°$)[27]. It can be also linked to the electromagnetic duality of the sphere: Zero backscattering is a property of objects that are dual symmetric and, additionally, have (discrete) rotational symmetry[12,13]. Mie theory provides an analytical expression for the backscattering efficiency as[10,28]

$$Q_b = \frac{1}{x^2}\left|\sum_{n=1}^{\infty}(2n+1)\ (-1)^n\ (a_n - b_n)\right|^2, \tag{1}$$

where n is the order of the multipole expansion associated with electric and magnetic Mie coefficients, a_n and b_n, respectively. The size parameter $x = 2\pi r/\lambda_0$ represents the ratio between the sphere radius r and the excitation wavelength λ_0. The backscattering efficiency depends on the terms $a_n - b_n$, which represent both the destructive interference between the electric and magnetic response of the sphere in the backward scattering direction, and also the breaking of electromagnetic duality by the sphere. For spheres, electromagnetic duality $\varepsilon_r = \mu_r$ is equivalent to having identical electrical and magnetic responses $a_n - b_n$ for all n, thus zero backscattering $Q_b = 0$.

Another important quantity to consider is the scattering efficiency Q_{sca}, which represents the ratio of the scattered energy in all directions to the energy incident upon the geometric cross section of the sphere. Achieving a vanishing backscattering would be pointless if no light is scattered at all. This quantity measures the strength of the interaction between the illumination and the sphere. The scattering efficiency is given by[27]

$$Q_{\mathrm{sca}} = \frac{2}{x^2}\sum_{\mathrm{n}=1}^{\infty}(2n+1)\ (|a_{\mathrm{n}}|^2 + |b_{\mathrm{n}}|^2). \tag{2}$$

In a nutshell, the broadband effect in the low permittivity regime is due to the approximate duality $a_{\mathrm{n}} \approx b_{\mathrm{n}}$, for all n, as we shall present in the next section. In this case, the sensitivity of the backscattering efficiency with respect to the electromagnetic size of the sphere diminishes. Thus, the ZBS regions become broadband and, despite the rather low permittivity, we show that there exists a parameter regime where the proposed spheres have also a considerable scattering efficiency. That's due to their rather large diameter, roughly between 1.55 and 3.1 times the wavelength.

Results

Theoretical concept: Backscattering behavior near duality. The main idea of this article is to employ the near-duality region of low permittivity to achieve a broadband suppression of backscattering. We will now analyze the sensitivity of the backscattering to changes in wavelength in this parameter regime. To this end, we employ the analytic expressions of the Mie coefficients.

The Mie coefficients of a sphere with arbitrary electric permittvity ε_{r} and magnetic permeability μ_{r} are given by[28,29]

$$a_n(x,\, m) = \frac{\psi_n(x)\psi'_n(mx) - \widetilde{m}\psi'_n(x)\psi_n(mx)}{\zeta_n^{(1)}(x)\psi'_n(mx) - \widetilde{m}\zeta_n^{(1)\prime}(x)\psi_n(mx)}, \tag{3}$$

$$b_{\mathrm{n}}(x,\, m) = \frac{\psi'_{\mathrm{n}}(x)\psi_{\mathrm{n}}(mx) - \widetilde{m}\psi_{\mathrm{n}}(x)\psi'_{\mathrm{n}}(mx)}{\zeta_{\mathrm{n}}^{(1)\prime}(x)\psi_{\mathrm{n}}(mx) - \widetilde{m}\zeta_{\mathrm{n}}^{(1)}(x)\psi'_{\mathrm{n}}(mx)}, \tag{4}$$

where m is the refractive index of the sphere relative to the ambient medium, assumed to be free space, and $\widetilde{m} = m/\mu_{\mathrm{r}}$. The prime represents the derivative of the function with respect to its argument. The functions $\psi_{\mathrm{n}}(x)$ and $\zeta_{\mathrm{n}}^{(1)}(x)$ are Riccati-Bessel functions defined in terms of the spherical Bessel and Hankel functions of the first kind, $j_{\mathrm{n}}(x)$ and $h_{\mathrm{n}}^{(1)}(x)$[30],

$$\psi_{\mathrm{n}}(x) = x\, j_{\mathrm{n}}(x),\ \zeta_{\mathrm{n}}^{(1)}(x) = x\, h_{\mathrm{n}}^{(1)}(x). \tag{5}$$

The sensitivity (V) of the backscattering efficiency with respect to wavelength changes (or more generally the size parameter x) can be defined as

$$V = \frac{\partial Q_{\mathrm{b}}(x)}{\partial x}. \tag{6}$$

Using that the differentiation of a square modulus of a complex function is given by the identity

$$\frac{\partial |f(x)|^2}{\partial x} = 2[\Re\{f(x)\}\Re\{f'(x)\} + \Im\{f(x)\}\Im\{f'(x)\}], \tag{7}$$

where $\Re\{\cdot\}$ and $\Im\{\cdot\}$ denote the real and imaginary parts of the arguments, respectively, we expand the derivative of the backscattering efficiency in Eq. (6)

$$\begin{aligned}\frac{\partial Q_b(x)}{\partial x} = \frac{2}{x^2}\Bigg\{&\sum_{\mathrm{n}=1}^{\infty}(2n+1)\ (-1)_{\mathrm{n}}\ \Re(a_{\mathrm{n}} - b_{\mathrm{n}})\ \sum_{l=1}^{\infty}(2l+1)\ (-1)_l\ \Re\left[\frac{\partial(a_l - b_l)}{\partial x}\right] \\ &+\sum_{\mathrm{n}=1}^{\infty}(2n+1)\ (-1)_n\ \Im(a_{\mathrm{n}} - b_{\mathrm{n}})\ \sum_{l=1}^{\infty}(2l+1)\ (-1)_l\ \Im\left[\frac{\partial(a_l - b_l)}{\partial x}\right]\Bigg\} \\ &-\frac{2}{x^3}\left|\sum_{\mathrm{n}=1}^{\infty}(2n+1)\ (-1)_n\ (a_{\mathrm{n}} - b_{\mathrm{n}})\right|^2,\end{aligned} \tag{8}$$

where n and l are positive integers. Accordingly, for low permittivity materials, i.e. near the duality point where $\widetilde{m} \to 1$, the limit of the backscattering sensitivity V defined in Eq. (6) depends on the following limits,

$$\lim_{\widetilde{m}\to 1}\ (a_n - b_n)\ (a_l - b_l), \tag{9}$$

$$\lim_{\widetilde{m}\to 1}\ (a_{\mathrm{n}} - b_{\mathrm{n}})\ \frac{\partial(a_l - b_l)}{\partial x}. \tag{10}$$

Using properties of limits, the limit of a product of functions is equal to the product of the limits of each function individually, if they both exist. The latter assumption is valid since Mie coefficients are bounded and continuous in the range [0,1]. Therefore, the backscattering sensitivity near the duality point vanishes if the terms $a_{\mathrm{n}} - b_{\mathrm{n}}$ tends to zero near the duality point. The terms $a_{\mathrm{n}} - b_{\mathrm{n}}$ turn out to be,

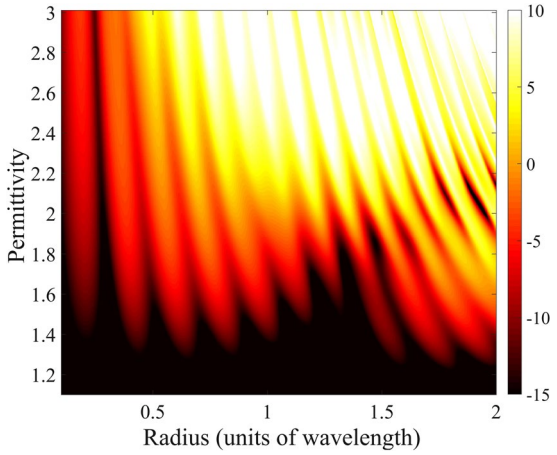

Figure 2. Backscattering efficiency Q_b [dB scale] of nonmagnetic spheres for a wide range of permittivities and radii. The black color indicates the regions of ZBS, which are broadband for low permittivity materials.

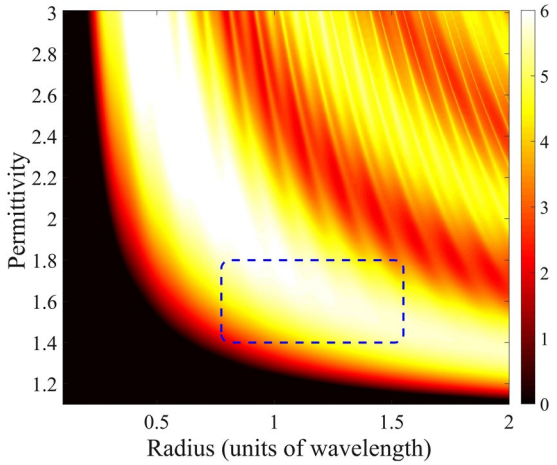

Figure 3. Scattering efficiency Q_{sca} [dB scale] of nonmagnetic spheres for a wide range of permittivities and radii. The white color indicates the regions of interest that show maximum interaction between the light and the sphere.

$$(a_n - b_n) = (1 - \widetilde{m}^2)\frac{\psi_n(x)\psi'_n(mx)\zeta_n^{(1)\prime}(x)\psi_n(mx) - \psi'_n(x)\psi_n(mx)\zeta_n^{(1)}(x)\psi'_n(mx)}{[\zeta_n^{(1)}(x)\psi'_n(mx) - \widetilde{m}\zeta_n^{(1)\prime}(x)\psi_n(mx)][\zeta_n^{(1)\prime}(x)\psi_n(mx) - \widetilde{m}\zeta_n^{(1)}(x)\psi'_n(mx)]}. \quad (11)$$

We note that the denominator of $a_n - b_n$ in Eq. (11) can't be zero since it is the product of the denominators of a_n and b_n [see Eqs (3) and (4)], and the Mie coefficients are bounded to the range [0,1]. Therefore, the value of Eq. (11) approaches zero as $\widetilde{m}$ approaches one, independently of both the multipolar order and the size parameter. Thus, the backscattering sensitivity near the duality point tends to zero ($V \to 0$). It identifies a regime that features the wavelength independent vanishing of the backscattering contributions for all multipolar orders n. This suggests a wavelength independent behavior, which leads to broadband backscattering suppression. This effect resembles the Kerker condition of ZBS but for nonmagnetic spheres made from low permittivity materials. Indeed, this is a regime of approximately duality: $a_n \approx b_n$ for all n.

Numerical evaluation: Parameter regime for broadband ZBS. Figure 2 shows the backscattering efficiency Q_b of a nonmagnetic sphere as a function of its radius and material permittivity. The dark regions in Fig. 2 represent vanishing backscattering. As predicted in the previous section, these ZBS regions get spectrally broadened for low values of the permittivity, i.e. in the near-duality region. These results suggest parameter regions of low permittivity for broadband ZBS.

Figure 3 shows Q_{sca} of the same nonmagnetic sphere again as a function of its radius and material permittivity. The white color indicates regions of a considerable scattering efficiency, which is a desired feature. Eventually, we are interested in minimizing the backscattering efficiency, while maximizing the scattering efficiency. In order to achieve both requirements, we investigate the backscattering ratio $R_b = Q_b/Q_{sca}$ for low permittivity spheres.

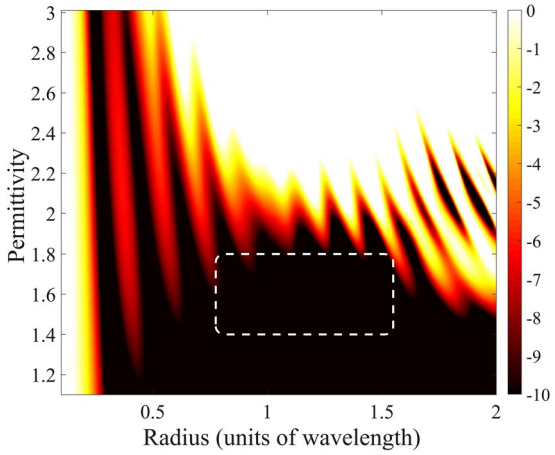

Figure 4. Backscattering ratio $R_b = Q_b/Q_{sca}$ [dB scale] of nonmagnetic spheres for a wide range of permittivities and radii. The dotted box indicates a broadband ZBS region that shows both a low backscattering ratio Q_b and a considerable scattering efficiency Q_{sca}.

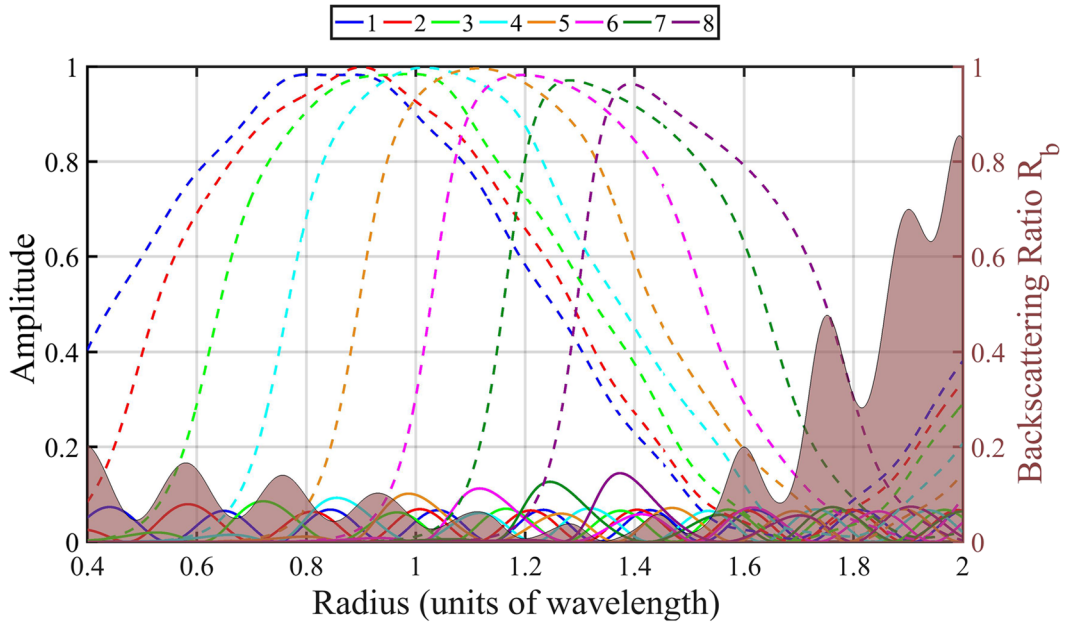

Figure 5. Solid area: Backscattering ratio R_b. Dashed lines: Scattering efficiency of each multipolar order $\frac{1}{2}(|a_n|^2 + |b_n|^2)$, for $n = 1 \ldots 8$. Solid lines: Duality breaking due to each multipolar order $|a_n - b_n|^2$.

Figure 4 shows that, as the permittivity decreases, low values of R_b are reached at first for a central range of wavelength-sized spheres.

The dotted box in Figs 3, 4 indicates an octave-wide spectral ZBS region for a radius between 0.775 and 1.55 in units of the wavelength, that shows both a backscattering ratio R_b below 10% (−10 dB) and a scattering efficiency Q_{sca} above 2 (3 dB). This is the most important finding of our article. We conclude that broadband backscattering suppression combined with a considerable scattering efficiency is possible using a wavelength-sized sphere made from a low permittivity material. An example for such material is Teflon[31] that exhibits a permittivity around 1.7 across the visible and near-IR spectra.

Discussion based on Mie coefficients

In order to further investigate this broadband effect, we use the Mie coefficients to analyze a nonmagnetic sphere of permittivity 1.7 for the radii corresponding to the region indicated in Fig. 4. Figure 5 displays the quantities

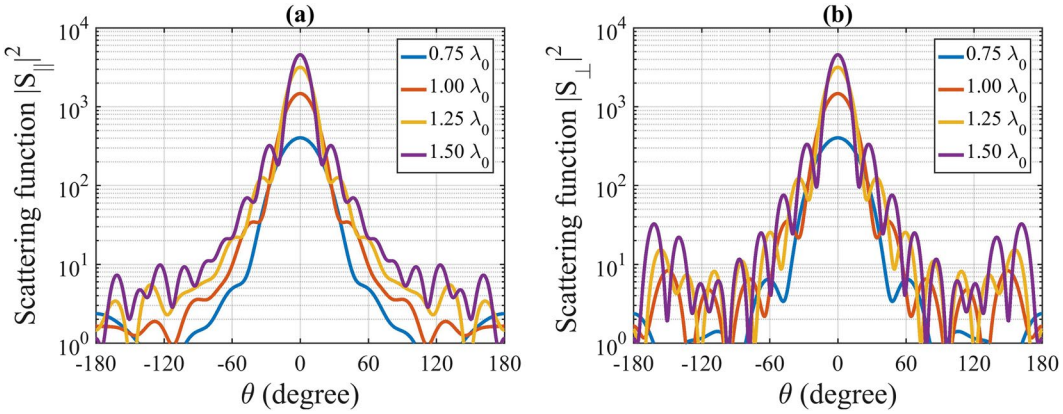

Figure 6. Angular distribution of the scattering functions (**a**) $|S_{\parallel}(\theta)|^2$ and (**b**) $|S_{\perp}(\theta)|^2$ of a nonmagnetic sphere of permittivity 1.7 for different radii. The scattering efficiency Q_{sca} values are 3.07, 3.8, 3.63, and 2.87 for radius/wavelength ratios of 0.75, 1.0, 1.25, and 1.5, respectively.

$$\frac{1}{2}(|a_n|^2 + |b_n|^2), \text{ and } |a_n - b_n|^2 \tag{12}$$

up to the eighth multipolar order. The first quantity in Eq. (12) is related to the scattering due to the n-th multipolar order (see Eq. (2)). The second quantity is the duality breaking due to the n-th multipolar order. It is easy to see that $|a_n - b_n|^2$ are the helicity changing terms that determine the numerator of the duality breaking measure introduced in Eq. 2 of ref.[32]. According to Eq. (1), these terms are related to ZBS in the sense that when $a_n = b_n$, the $n-$ th multipolar order does not contribute to the backward scattering.

Figure 5 shows low duality breaking for all multipolar orders across a wide range. This matches the analytical result obtained previously: Broadband backscattering suppression due to wavelength independent approximate duality $a_n \approx b_n$. Additionally, the scattering due to each multipolar term reaches its maximum (resonant) value inside the 0.775–1.55 band, and many have simultaneously large values in this region. This last feature is consistent with wide resonances characteristic of low refractive indexes.

In order to investigate the scattering pattern, Fig. 6 shows the scattering functions[28] $|S_{\parallel}(\theta)|^2$ and $|S_{\perp}(\theta)|^2$ of the parallel and perpendicular polarizations, where θ is the angle in the scattering plane that contains the wavevector of the illumination and the observer. The proposed sphere of permittivity 1.7 clearly exhibits a dominant directional scattering pattern in the forward direction (around $\theta = 0^{\circ}$) for the considered octave frequency band, for both polarizations. To quantify the scattering pattern, the asymmetry parameter g is evaluated, which indicates the value of the average cosine of the distribution of scattering angle[28]

$$g = <u> = \frac{1}{x^2\ Q_{sca}} \int_{-1}^{1} (|S_{\parallel}|^2 + |S_{\perp}|^2)\, u\ du, \tag{13}$$

where $u = \cos(\theta)$. The asymmetry parameter is bounded by $[-1, 1]$. If the sphere scatters light equally between the forward and backward hemisphere, g is zero. For forward scattering pattern, g is positive. For spherical objects, the asymmetry parameter g is independent of the polarization state. For the scattering patterns represented in Fig. 6, the asymmetry parameter values are around 0.85. Hence, the scattered energy is concentrated in a solid angle of 35°.

In conclusion, we have shown that electromagnetically large nonmagnetic spheres made from low permittivity materials exhibit a notable number of closely packed multipole resonances where both the electric and magnetic multipolar moments have comparable complex amplitudes $a_n \approx b_n$ for all n. Therefore, the electromagnetic duality is approximately met in a broadband fashion even though the materials are nonmagnetic. This results in a broadband backscattering suppression accompanied with a considerable scattering efficiency. In other words, the existence of significant higher order multipolar moments in these large spheres of low permittivity enhances the broadband effect, in stark contrast to high permittivity spheres, where terms higher than the dipoles typically degrade the ZBS performance. This result motivates further analysis on the use of dielectric spheres of low permittivity in all-dielectric metamaterials, for instance, to enhance the solar cell efficiency as an alternative to metallic nanoparticles that suffer from intrinsic losses[7].

Methods

The analysis is performed using a freely available Mie code[33] to compute the Mie coefficients of the sphere: a_n and b_n. Using the Mie coefficients, the scattering efficiency Q_{sca}, the backscattering efficiency Q_b, the angular scattering functions $S_{\parallel}$ and $S_{\perp}$ (elements of the scattering matrix), and the asymmetry parameter g can be computed. The Wiscombe criterion has been used to guarantee convergence of all the shown quantities[34,35]. The analysis is done

using lengths in units of the wavelength. This allows to easily scale the results to any desired spectral region as long as there are materials available with the required properties.

References

1. Mie, G. Beiträge zur Optik trüber Medien, speziell kolloidaler Metallösungen. *Annalen der physik* **330**, 377–445 (1908).
2. Alu, A. & Engheta, N. Tuning the scattering response of optical nanoantennas with nanocircuit loads. *Nat. Photon.* **2**, 307–310 (2008).
3. Knoll, B. & Keilmann, F. Enhanced dielectric contrast in scattering-type scanning near-field optical microscopy. *Opt. Commun.* **182**, 321–328 (2000).
4. Moreno, F., Albella, P. & Nieto-Vesperinas, M. Analysis of the spectral behavior of localized plasmon resonances in the near-and far-field regimes. *Langmuir* **29**, 6715–6721 (2013).
5. Sarmecanic, J., Fomenkova, M., Jones, B. & Lavezzi, T. Constraints on the nucleus and dust properties from mid-infrared imaging of comet hyakutake. *Astrophys. J. Lett.* **483**, L69 (1997).
6. Ferry, V. E., Munday, J. N. & Atwater, H. A. Design considerations for plasmonic photovoltaics. *Adv. Mater.* **22**, 4794–4808 (2010).
7. Akimov, Y. A., Koh, W., Sian, S. & Ren, S. Nanoparticle-enhanced thin film solar cells: Metallic or dielectric nanoparticles? *Appl. Phys. Lett.* **96**, 073111 (2010).
8. Zhang, Y., Nieto-Vesperinas, M. & Sáenz, J. J. Dielectric spheres with maximum forward scattering and zero backscattering: a search for their material composition. *J. Opt.* **17**, 105612 (2015).
9. Chen, J., Ng, J., Lin, Z. & Chan, C. Optical pulling force. *Nat. Photon.* **5**, 531–534 (2011).
10. Kerker, M., Wang, D.-S. & Giles, C. Electromagnetic scattering by magnetic spheres. *J. Opt. Soc. Am.* **73**, 765–767 (1983).
11. Fernandez-Corbaton, I. *et al*. Electromagnetic duality symmetry and helicity conservation for the macroscopic maxwell's equations. *Phys. Rev. Lett.* **111**, 060401 (2013).
12. Zambrana-Puyalto, X., Fernandez-Corbaton, I., Juan, M. L., Vidal, X. & Molina-Terriza, G. Duality symmetry and kerker conditions. *Opt. Lett.* **38**, 1857–1859 (2013).
13. Fernandez-Corbaton, I. Forward and backward helicity scattering coefficients for systems with discrete rotational symmetry. *Opt. Express* **21**, 29885–29893 (2013).
14. Kuznetsov, A., Miroshnichenko, A., Fu, Y., Zhang, J. & Luk'yanchuk, B. Magnetic light. *Sci. Rep.* **2**, 492 (2012).
15. Evlyukhin, A. B., Reinhardt, C., Seidel, A., Luk'yanchuk, B. S. & Chichkov, B. N. Optical response features of Si-nanoparticle arrays. *Phys. Rev. B* **82**, 045404 (2010).
16. Garca-Etxarri, A. *et al*. Strong magnetic response of submicron silicon particles in the infrared. *Opt. Express* **19**, 4815–4826 (2011).
17. Zambrana-Puyalto, X., Vidal, X., Juan, M. L. & Molina-Terriza, G. Dual and anti-dual modes in dielectric spheres. *Opt. Express* **21**, 17520–17530 (2013).
18. Geffrin, J.-M. *et al*. Magnetic and electric coherence in forward-and back-scattered electromagnetic waves by a single dielectric subwavelength sphere. *Nat. Commun.* **3**, 1171 (2012).
19. Fu, Y. H., Kuznetsov, A. I., Miroshnichenko, A. E., Yu, Y. F. & Luk'yanchuk, B. Directional visible light scattering by silicon nanoparticles. *Nat. Commun.* **4**, 1527 (2013).
20. Zhang, S. *et al*. Colloidal moderate-refractive-index cu2o nanospheres as visible-region nanoantennas with electromagnetic resonance and directional light-scattering properties. *Adv. Mater.* **27**, 7432–7439 (2015).
21. Person, S. *et al*. Demonstration of zero optical backscattering from single nanoparticles. *Nano Lett.* **13**, 1806–1809 (2013).
22. Staude, I. *et al*. Tailoring directional scattering through magnetic and electric resonances in subwavelength silicon nanodisks. *ACS Nano* **7**, 7824–7832 (2013).
23. Decker, M. *et al*. High-efficiency dielectric huygens surfaces. *Adv. Opt. Mater.* **3**, 813–820 (2015).
24. Alaee, R., Filter, R., Lehr, D., Lederer, F. & Rockstuhl, C. A generalized kerker condition for highly directive nanoantennas. *Opt. Lett.* **40**, 2645–2648 (2015).
25. Li, Y. *et al*. Broadband zero-backward and near-zero-forward scattering by metallo-dielectric core-shell nanoparticles. *Sci. Rep.* **5**, 12491 (2014).
26. Luk'yanchuk, B. S., Paniagua-DomÍnguez, R., Minin, I., Minin, O. & Wang, Z. Refractive index less than two: photonic nanojets yesterday, today and tomorrow. *Opt. Mater. Express* **7**, 1820–1847 (2017).
27. Kerker, M. *The scattering of light and other electromagnetic radiation* (Elsevier, 2016).
28. Bohren, C. F. & Huffman, D. R. *Absorption and Scattering of Light by Small Particles* (John Wiley & Sons, 2008).
29. Grainger, R. G., Lucas, J., Thomas, G. E. & Ewen, G. B. Calculation of mie derivatives. *Appl. Opt.* **43**, 5386–5393 (2004).
30. Abramowitz, M. & Stegun, I. A. *Handbook of mathematical functions: with formulas, graphs, and mathematical tables*, vol. 55 (Courier Corporation, 1964).
31. Yang, M. K., French, R. H. & Tokarsky, E. W. Optical properties of teflon af amorphous fluoropolymers. *J. Micro/Nanolith. MEMS MOEMS* **7**, 033010 (2008).
32. Fernandez-Corbaton, I., Fruhnert, M. & Rockstuhl, C. Dual and chiral objects for optical activity in general scattering directions. *ACS Photonics* **2**, 376–384 (2015).
33. Mätzler, C. Matlab functions for mie scattering and absorption, version 2. *IAP Res. Rep* **8**, 1–24 (2002).
34. Wiscombe, W. J. Improved mie scattering algorithms. *Appl. Opt.* **19**, 1505–1509 (1980).
35. Allardice, J. R. & Le R, E. C. Convergence of mie theory series: criteria for far-field and near-field properties. *Appl. Opt.* **53**, 7224–7229 (2014).

Acknowledgements

We acknowledge support by the DFG and Open Access Publishing Fund of Karlsruhe Institute of Technology. This work has been partly funded by the German Science Foundation within the priority program SPP1839 Tailored Disorder (RO 3640/7-1).

Author Contributions

M.I.A. discovered and analyzed the approximate duality regime of low permittivity spheres of large sizes in the research context of ZBS from approximately dual objects provided by I.F-C and C.R. C.R. and I.F-C. supervised and guided the study and contributed to the scientific discussion. M.I.A lead the writing of the article, with contributions from I.F-C and C.R.

Additional Information

Competing Interests: The authors declare that they have no competing interests.

Publisher's note: Springer Nature remains neutral with regard to jurisdictional claims in published maps and institutional affiliations.